

**Brain-region specific susceptibility of Lewy body pathology in synucleinopathies
is governed by α -synuclein conformations.**

Authors

Laura de Boni^{1,2}, Aurelia Hays Watson¹, Ludovica Zaccagnini¹, Amber Wallis¹, Kristina Zhelcheska³, Nora Kim⁴,
John Sanderson⁵, Haiyang Jiang⁶, Elodie Martin¹, Adam Cantlon⁶, Matteo Rovere⁷, Lei Liu⁶, Marc Sylvester⁸,
Tammaryn Lashley⁹, Ulf Dettmer⁶, Zane Jaunmuktane^{9,10,11}, Tim Bartels^{1*}

Correspondence to: t.bartels@ucl.ac.uk

This online resource includes the following files:

Figures 1 to 15
Table 1

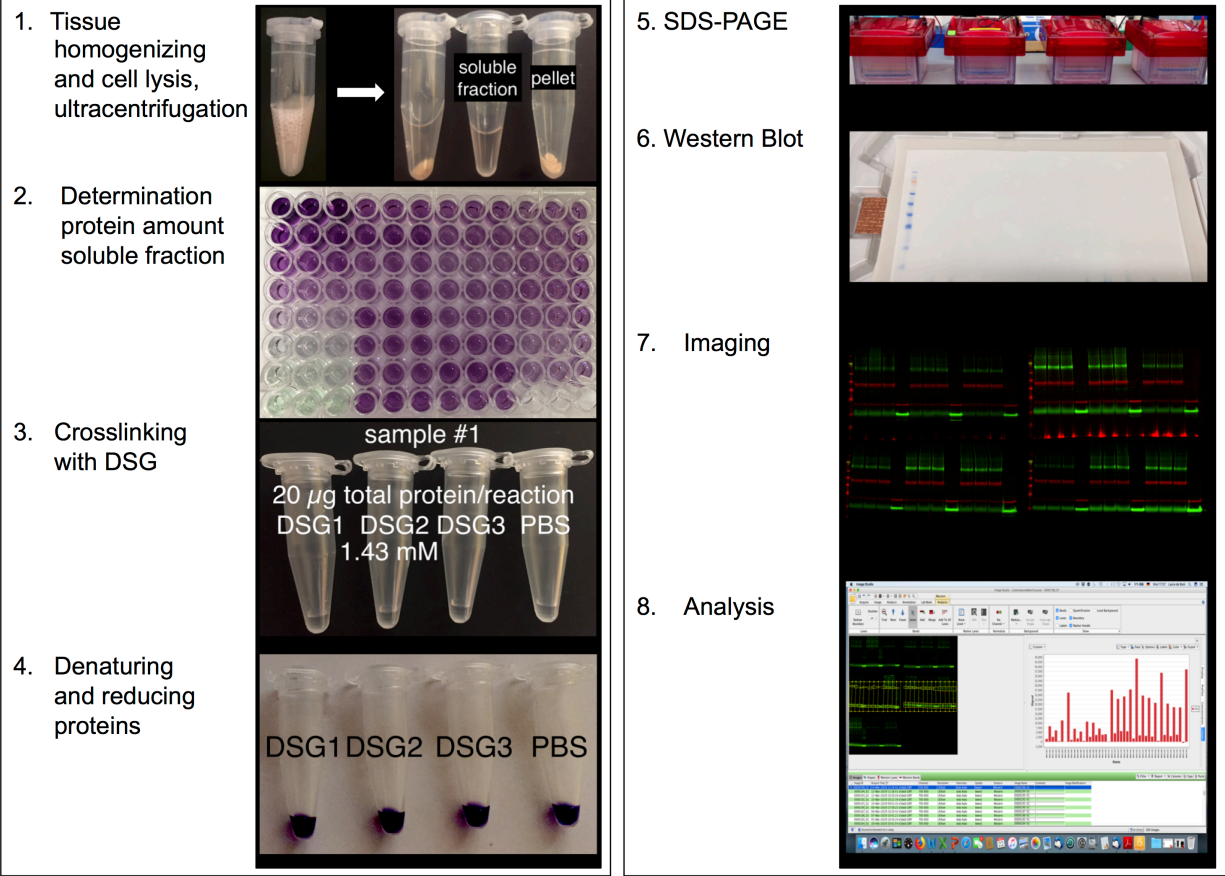


Fig. 1 Crosslinking protocol for tissue and cell lysates. Protocol and workflow of the crosslinking protocol using tissue and cell lysates. The procedure is described in the Methods section.

Increasing sonication amplitude [%] decreases αS^H / αS^U ratio

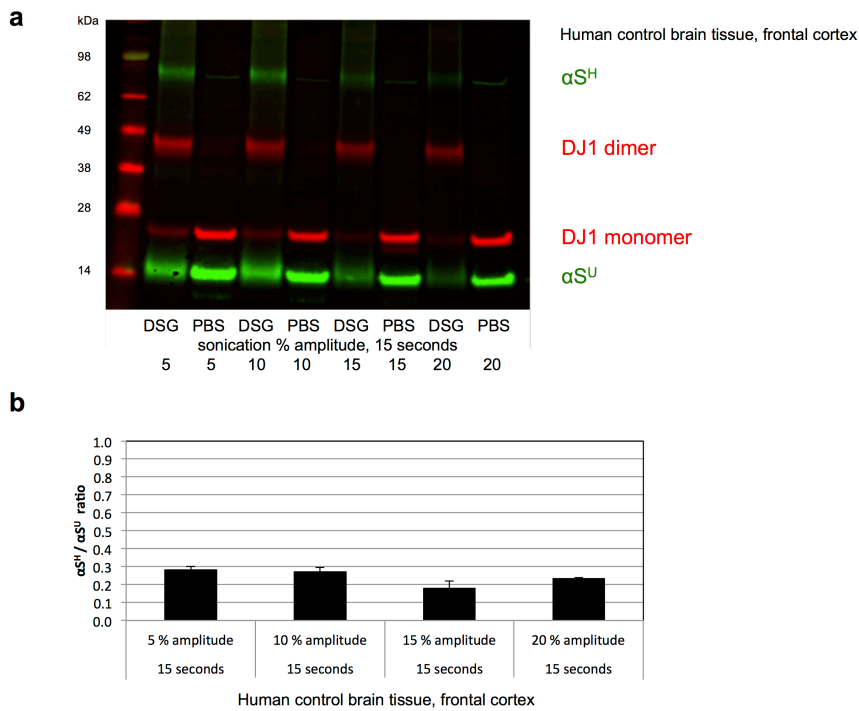
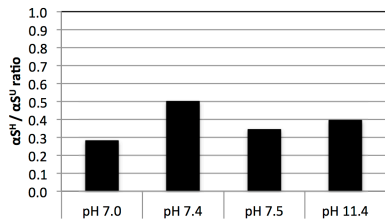


Fig. 2 Validation of the crosslinking protocol. The procedure is described in the Methods section. **a** Western blot and **b** quantification of the Western blot of crosslinked (DSG) human control brain tissue (frontal cortex, n=1) subjected to different sonication amplitudes (Fisher Scientific Model 705 Sonic Dismembrator 5 %, 10 %, 15 %, 20 %). Non-crosslinked samples (PBS) are displayed in **a**. αS^H are sensitive to sonication as described previously¹ and sonication settings were chosen accordingly (Sonic Dismembrator model 300 settings 40, 15 seconds, Fisher Scientific Model 705 Sonic Dismembrator 5 % of amplitude 15 seconds). Green = αS , red = DJ1

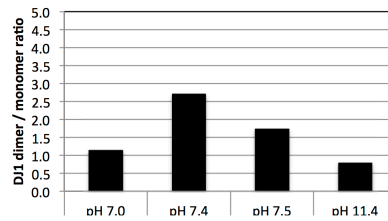
Efficient crosslinking reaction at neutral pH
a1 $\alpha S^H / \alpha S^U$ ratio

Human control brain tissue, frontal cortex



a2 DJ1 dimer / monomer ratio

Human control brain tissue, frontal cortex



b Optimal αS^H detection using 1.4 mM DSG f.c.

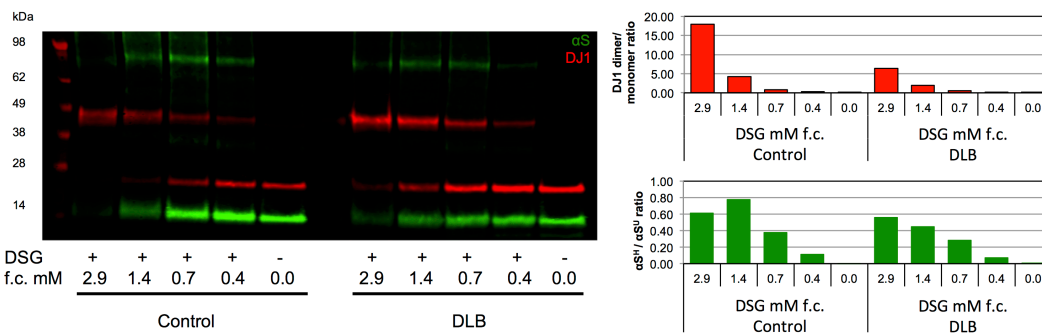


Fig. 3 Validation of the crosslinking protocol. The procedure is described in the Methods section. **a1** Quantification of $\alpha S^H / \alpha S^U$ ratios and **a2** DJ1 dimer / monomer ratios in human control brain tissue (frontal cortex, n=1) depending on different pH concentrations. 1x PBS has been used at different pH for solubilization of DSG and for filling up the sample volume to 25 μ l total volume. Efficient crosslinking (controlled by DJ1) is carried out at pH 7.4. **b** Western blot with quantifications of crosslinked human control and DLB brain tissue (frontal cortex, n=1 each). The crosslinking reaction is depending on the amount and final concentration of the crosslinker DSG. Thus, for the crosslinking protocol for frozen brain tissue and cell pellets, a final concentration (f.c.) of 1.4 mM DSG was chosen. DSG “+“ = crosslinked sample, DSG “-“ = non-crosslinked (control) sample. Green = αS , red = DJ1

Dependence of crosslinking reaction on total protein amounts

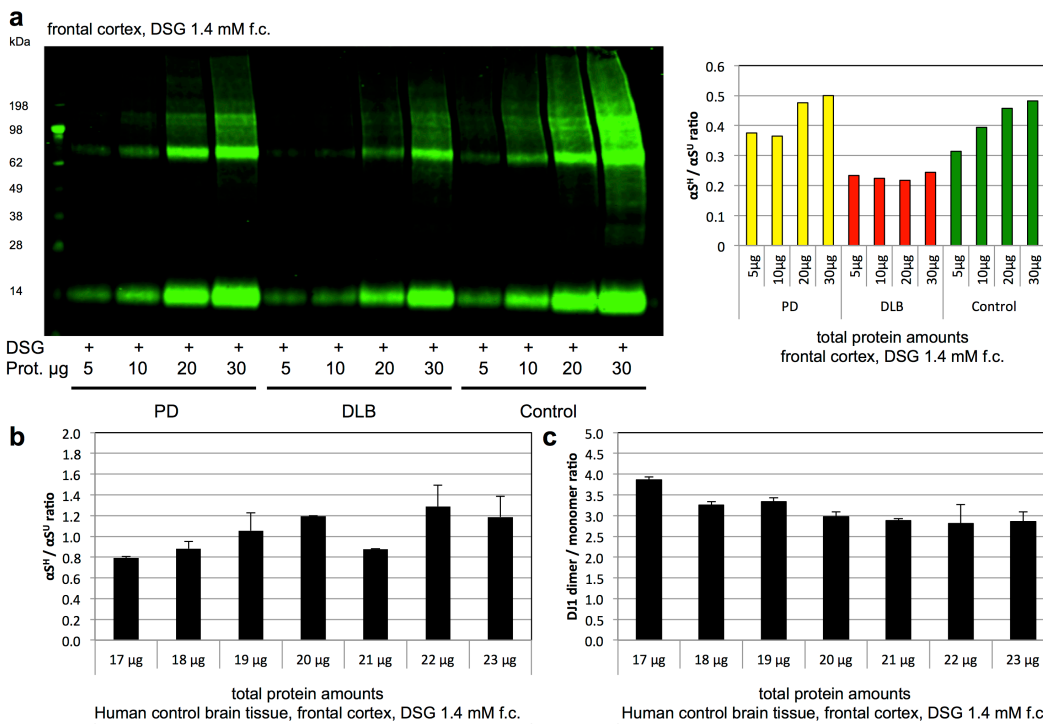


Fig. 4 Validation of the crosslinking protocol. The procedure is described in the Methods section. **a** Western blot and quantification demonstrating the efficiency of the crosslinking reaction (human brain tissue: control, DLB, PD (n=1 each), frontal cortex) depending on the total amount of protein input (5 µg, 10 µg, 20 µg, 30 µg) into the reaction and the failure to detect higher amounts of αS^H in DLB despite a higher total protein input. DSG “+” = crosslinked sample. **b**, **c** Minor changes in total protein input (17 µg, 18 µg, 19 µg, 20 µg, 21 µg, 22 µg, 23 µg) exhibit very similar crosslinking results and efficiency (controlled by DJ1). Human brain tissue, frontal cortex (n=1). F. c. = final concentration.

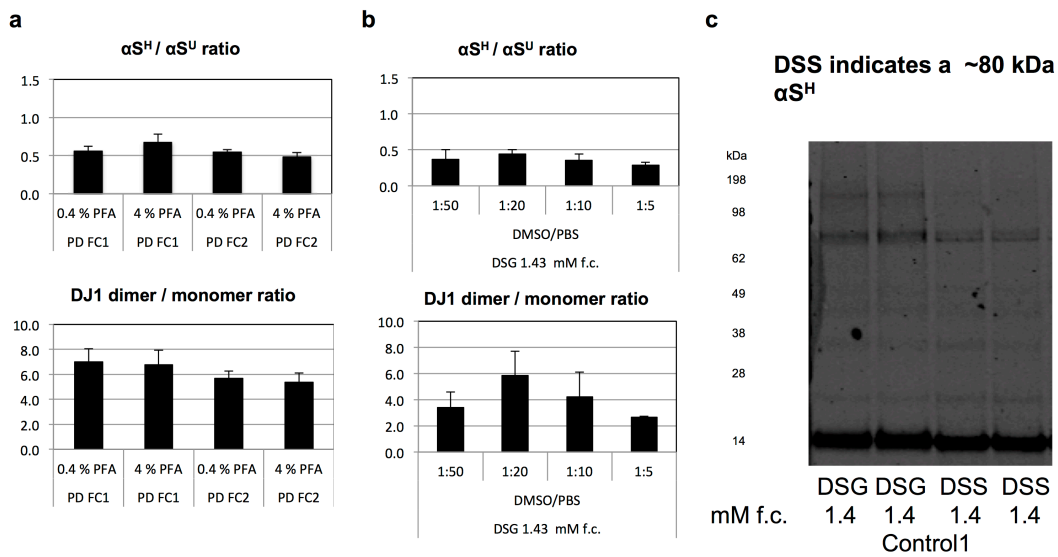


Fig. 5 Validation of the crosslinking protocol. The procedure is described in the Methods section. **a** Comparison of different PFA concentrations for the fixation of αS . Similar $\alpha S^H / \alpha S^U$ ratios (A) and DJ1 dimer / monomer ratios upon fixation with PFA 0.4 % or PFA 4 %. Samples have been analyzed in biological duplicates. **b** DMSO does not lead to an artificial oligomer formation. DSG was solubilized in different amounts of DMSO and added to a protein lysate from frontal cortex control brain tissue. The crosslinking reaction seems to be most efficient at a DSG PBS/DMSO ratio of 1:20. This ratio is used in the crosslinking protocol. PD = Parkinson's disease, FC = frontal cortex. **c** The procedure for the crosslinking is described in the Methods section. Western blot displaying control (n=1) human brain tissue, frontal cortex, crosslinked (technical duplicates) with either DSG or disuccinimidyl suberate (DSS). DSS detects αS^H migrating at ~80 kDa in accordance with DSG. All crosslinkers have been used at a final concentration (f.c.) of 1.4 mM in human brain tissue.

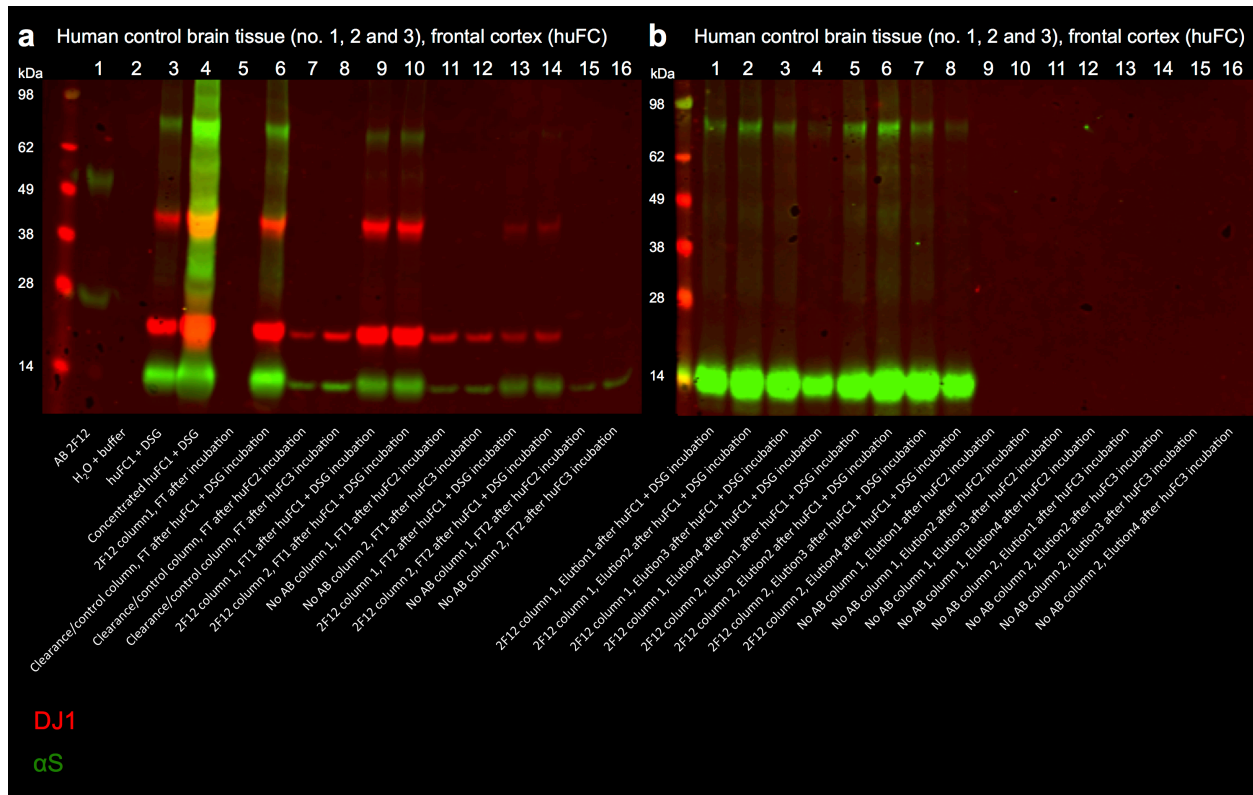


Fig. 6 Immunoprecipitation of α S from human post-mortem native brain tissue. The procedure is described in the Methods section. Samples: 3 different human control brain tissues (no. 1, 2, 3), frontal cortex. The crosslinking procedure is performed as described in the Methods section. **a** Lane 1: Displaying the applied anti- α S 2F12 antibody (25 kDa light and 50 kDa heavy chain). Lane 2: Used 1x conditioning buffer without artificial protein detection. Lane 3: Crosslinked human brain lysate (no. 1) displaying α S^H and α S^U (green) and DJ1 dimer and monomer (red). Lane 4: Concentrated crosslinked human brain lysate (no. 1). Lane 5: Flow through (FT) after clearing of the column (AminoLink Plus™ Coupling Resin) incubated with the 2F12 antibody demonstrating complete binding of the 2F12 antibody. Lane 6: FT after incubation of the crosslinked sample no. 1 on the control/clearance column (Pierce Control Agarose Resin, non-amine reactive). Lane 7: FT after incubation of the non-crosslinked sample no. 2 on the control/clearance column. Lane 8: FT after incubation of the non-crosslinked sample no. 3 on the control/clearance column. Lane 9: FT after incubation of the crosslinked sample no. 1 on the 2F12 antibody column. Column is saturated and some protein lost during the washing step. Lane 10: FT after incubation of the crosslinked sample no. 1 on another 2F12 antibody column. Lane 11: FT of column incubated without any antibody and sample no. 3. Lane 13: Second FT after incubation of the crosslinked sample no. 1 on the 2F12 antibody column. Column is saturated and some protein lost during the washing step. Lane 14: Second FT after incubation of the crosslinked sample no. 1 on another 2F12 antibody column. Lane 15: Second FT of column incubated without any antibody and sample no. 2. Lane 16: Second FT of column incubated without any antibody and sample no. 3. **b** Lane 1-4: Elution fractions 1-4 of 2F12 column no. 1 incubated with the crosslinked brain sample no 1 showing the purification of the α S protein (absence of DJ1 protein). Lane 5-8: Elution fractions 1-4 of 2F12 column no. 2 incubated with the crosslinked brain sample no. 1 showing the purification of the α S protein (absence of DJ1 protein). Lane 9-12: Elution fractions 1-4 of one column without antibody incubated with the non-crosslinked brain sample no 2. No protein binding to the column, no elution of protein in the final elution steps. Lane 13-16: Elution fractions 1-4 of a second column without antibody incubated with the non-crosslinked brain sample no 3. No protein binding to the column, no elution of protein in the final elution steps. Green = α S, red = DJ1

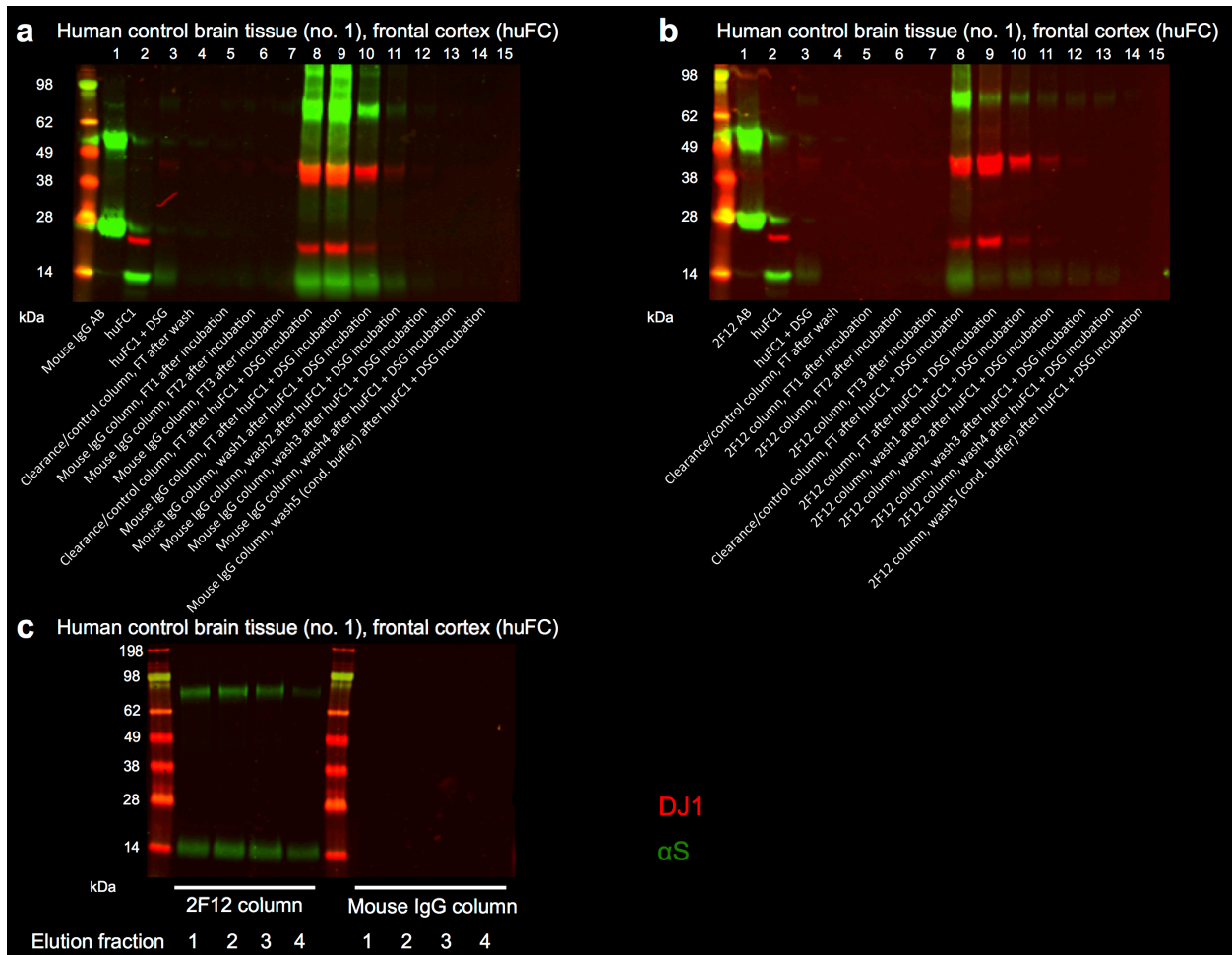


Fig. 7 Immunoprecipitation of α S from human post-mortem native brain tissue. The procedure is described in the Methods section. Sample: human control brain tissues (no. 1), frontal cortex. The crosslinking is performed according to the procedure described in the Methods section. **a** Lane 1: Displaying the applied mouse IgG (25 kDa light and 50 kDa heavy chain) used as a control antibody. Lane 2: non-crosslinked lysate human brain tissue no. 1. Slight overflow from Lane 1. Lane 3: Crosslinked lysate human brain tissue no. 1. Lane 4: Flow Through (FT) of the washed clearance/control column (Pierce Control Agarose Resin, non-amine reactive); no protein detection. Lane 5-8: FTs after incubation of the antibody column (AminoLink Plus™ Coupling Resin) with the mouse IgG demonstrating complete binding of the mouse IgG. Lane 8: FT after incubation of the clearance/control column with the crosslinked human brain lysate no. 1. Lane 9: FT after incubation of the mouse IgG antibody column with the crosslinked human brain lysate no. 1. Lane 10-15: FT after the washing steps of the mouse IgG antibody column incubated with the crosslinked human brain lysate no. 1. **b** Lane 1: Displaying the applied anti- α S antibody (25 kDa light and 50 kDa heavy chain). Lane 2: Non-crosslinked lysate human brain tissue no. 1. Slight overflow from lane 1. Lane 3: Crosslinked lysate human brain tissue no. 1. Lane 4: Flow Through (FT) of the washed clearance/control column (Pierce Control Agarose Resin, non-amine reactive); no protein detection. Lane 5-8: FTs after incubation of the antibody column (AminoLink Plus™ Coupling Resin) with the 2F12 antibody demonstrating complete binding of the 2F12. Lane 8: FT after incubation of the clearance/control column with the crosslinked human brain lysate no. 1. Lane 9: FT after incubation of the 2F12 antibody column with the crosslinked human brain lysate no. 1. Column is saturated, no complete binding of the crosslinked lysate. Lane 10-15: FT after the washing steps of the 2F12 antibody column incubated with the crosslinked human brain lysate no. 1. **c** Lane 1-4 2F12 column: Elution fractions 1-4 of 2F12 column incubated with the crosslinked brain sample no. 1 showing the purification of the α S protein (absence of DJ1 protein). Lane 1-4 mouse IgG column: Elution fractions 1-4 of mouse IgG column incubated with the crosslinked brain sample no. 1 showing no binding and accordingly no elution of α S protein or DJ1. Green = α S, red = DJ1

Table 1 Mass Spectrometry results of purified α S from multiple sources

α S sample (gel piece)	Accession	Description	Protein Group IDs	Coverage [%]	Unique Peptides	Protein Unique Peptides	AAs	MW [kDa]	calc. pI	Abundances	Gene Symbol
mock 14 kDa	P81605	Dermicidin	11	20	3	3	110	11.3	6.54	7.3E+06	DCD
mock 14 kDa	Q86YZ3	Hornerin	4	1	2	2	2850	282.2	10.04	5.7E+06	HRNR
mock 14 kDa	P37840	α -Synuclein	12	21	4	2	140	14.5	4.7	2.4E+06	SNCA
α S cytosolic unfolded, 14 kDa	P37840	α -Synuclein	19	40	9	5	140	14.5	4.7	2.8E+07	SNCA
α S cytosolic unfolded, 14 kDa	Q86YZ3	Hornerin	5	3	3	3	2850	282.2	10.04	2.0E+07	HRNR
α S cytosolic unfolded, 14 kDa	P14923	Junction plakoglobin	16	4	3	3	745	81.7	6.14	6.9E+06	JUP
α S cytosolic unfolded, 14 kDa	P15924	Desmoplakin	13	1	5	5	2871	331.6	6.81	3.0E+06	DSP
α S cytosolic unfolded, 14 kDa	P81605	Dermicidin	18	12	3	3	110	11.3	6.54	1.7E+06	DCD
mock 80 kDa	P37840	α -Synuclein	24	52	12	9	140	14.5	4.7	1.3E+08	SNCA
mock 80 kDa	Q86YZ3	Hornerin	8	3	2	2	2850	282.2	10.04	1.7E+07	HRNR
mock 80 kDa	P0DMV8	Heat shock 70 kDa protein	21	14	5	1	641	70	5.66	7.2E+06	HSPA1B; HSPA1A
mock 80 kDa	P15924	Desmoplakin	17	1	3	3	2871	331.6	6.81	1.5E+06	DSP
mock 80 kDa	P81605	Dermicidin	23	21	2	2	110	11.3	6.54	4.9E+05	DCD
α S cytosolic helical, 80 kDa	P0DMV8	Heat shock 70 kDa protein 1A	172	89	43	43	641	70	5.66	1.6E+11	HSPA1B; HSPA1A
α S cytosolic helical, 80 kDa	P11021	Endoplasmic reticulum chaperone BiP	151	57	40	40	654	72.3	5.16	1.9E+10	HSPA5
α S cytosolic helical, 80 kDa	P37840	α -Synuclein	200	81	11	9	140	14.5	4.7	1.1E+10	SNCA
α S cytosolic helical, 80 kDa	P11142	Heat shock cognate 71 kDa protein	128	59	25	25	646	70.9	5.52	6.7E+09	HSPA8
α S cytosolic helical, 80 kDa	P38646	Stress-70 protein, mitochondrial	205	44	25	25	679	73.6	6.16	2.2E+09	HSPA9
α S cytosolic helical, 80 kDa	P14136	Glial fibrillary acidic protein	32	6	1	1	432	49.9	5.52	1.4E+09	GFAP
α S cytosolic helical, 80 kDa	P04406	Glyceraldehyde-3-phosphate dehydrogenase	147	59	14	13	335	36	8.46	5.2E+08	GAPDH
α S cytosolic helical, 80 kDa	P40926	Malate dehydrogenase, mitochondrial	99	30	7	7	338	35.5	8.68	3.3E+08	MDH2
α S cytosolic helical, 80 kDa	P13667	Protein disulfide-isomerase A4	34	25	13	13	645	72.9	5.07	3.0E+08	PDIA4
α S cytosolic helical, 80 kDa	P15924	Desmoplakin	113	8	23	23	2871	331.6	6.81	1.9E+08	DSP
α S cytosolic helical, 80 kDa	P49915	GMP synthase	70	15	7	7	693	76.7	6.87	1.6E+08	GMPS
α S cytosolic helical, 80 kDa	Q5D862	Filaggrin-2	106	2	5	5	2391	247.9	8.31	1.6E+08	FLG2
α S cytosolic	P31944	Caspase-14	5	30	7	7	242	27.7	5.58	1.5E+08	CASP14

helical, 80 kDa												
α S cytosolic helical, 80 kDa	Q12931	Heat shock protein 75 kDa, mitochondrial	112	17	8	8	704	80.1	8.21	1.5E+08	TRAP1	
α S cytosolic helical, 80 kDa	Q02413	Desmoglein-1	108	17	12	12	1049	113.7	5.03	1.4E+08	DSG1	
α S cytosolic helical, 80 kDa	P07237	Protein disulfide-isomerase	96	31	11	11	508	57.1	4.87	1.0E+08	P4HB	
α S cytosolic helical, 80 kDa	P10809	60 kDa heat shock protein, mitochondrial	207	21	7	7	573	61	5.87	8.6E+07	HSPD1	
α S cytosolic helical, 80 kDa	Q5T750	Skin-specific protein 32	211	4	2	2	250	26.2	7.97	7.5E+07	C1orf68	
α S cytosolic helical, 80 kDa	P17066	Heat shock 70 kDa protein 6	75	22	3	3	643	71	6.14	7.1E+07	HSPA6	
α S cytosolic helical, 80 kDa	P08133	Annexin A6	11	27	15	15	673	75.8	5.6	7.1E+07	ANXA6	
α S cytosolic helical, 80 kDa	P07355	Annexin A2	145	37	12	4	339	38.6	7.75	6.5E+07	ANXA2	
α S cytosolic helical, 80 kDa	Q08554	Desmocollin-1	246	7	5	5	894	99.9	5.43	5.2E+07	DSC1	
α S cytosolic helical, 80 kDa	P07195	L-lactate dehydrogenase B chain	137	22	7	7	334	36.6	6.05	5.1E+07	LDHB	
α S cytosolic helical, 80 kDa	P50395	Rab GDP dissociation inhibitor beta	226	28	5	5	445	50.6	6.47	5.1E+07	GDI2	
α S cytosolic helical, 80 kDa	Q15181	Inorganic pyrophosphatase	63	21	4	4	289	32.6	5.86	5.0E+07	PPA1	
α S cytosolic helical, 80 kDa	Q15084	Protein disulfide-isomerase A6	210	9	2	2	440	48.1	5.08	4.7E+07	PDIA6	
α S cytosolic helical, 80 kDa	P14923	Junction plakoglobin	153	12	8	7	745	81.7	6.14	4.5E+07	JUP	
α S cytosolic helical, 80 kDa	P07900	Heat shock protein HSP 90-alpha	43	15	5	4	732	84.6	5.02	4.3E+07	HSP90AA1	
α S cytosolic helical, 80 kDa	P17812	CTP synthase 1	248	17	8	8	591	66.6	6.46	4.1E+07	CTPS1	
α S cytosolic helical, 80 kDa	Q92945	Far upstream element-binding protein 2	146	3	2	2	711	73.1	7.3	4.0E+07	KHSRP	
α S cytosolic helical, 80 kDa	P14618	Pyruvate kinase PKM	222	17	6	5	531	57.9	7.84	3.5E+07	PKM	
α S cytosolic helical, 80 kDa	P23526	Adenosylhomocysteinase	184	9	4	4	432	47.7	6.34	3.4E+07	AHCY	
α S cytosolic helical, 80 kDa	P00338	L-lactate dehydrogenase A chain	171	14	4	4	332	36.7	8.27	3.3E+07	LDHA	
α S cytosolic helical, 80 kDa	P29401	Transketolase	102	12	5	5	623	67.8	7.66	2.9E+07	TKT	
α S cytosolic helical, 80 kDa	P19623	Spermidine synthase	141	8	3	3	302	33.8	5.49	2.6E+07	SRM	
α S cytosolic helical, 80 kDa	P13797	Plastin-3	203	17	9	6	630	70.8	5.6	2.6E+07	PLS3	
α S cytosolic helical, 80 kDa	P40925	Malate dehydrogenase, cytoplasmic	216	13	3	3	334	36.4	7.36	2.6E+07	MDH1	
α S cytosolic helical, 80 kDa	Q13867	Bleomycin hydrolase	193	5	2	2	455	52.5	6.27	2.6E+07	BLMH	
α S cytosolic helical, 80 kDa	P00491	Purine nucleoside phosphorylase	185	34	7	7	289	32.1	6.95	2.5E+07	PNP	

α S cytosolic helical, 80 kDa	P05089	Arginase-1	158	22	5	5	322	34.7	7.21	2.2E+07	ARG1
α S cytosolic helical, 80 kDa	P06733	Alpha-enolase	206	14	4	3	434	47.1	7.39	2.1E+07	ENO1
α S cytosolic helical, 80 kDa	P14625	Endoplasmic	15	11	6	4	803	92.4	4.84	2.1E+07	HSP90B1
α S cytosolic helical, 80 kDa	P54652	Heat shock-related 70 kDa protein 2	92	38	8	8	639	70	5.74	2.0E+07	HSPA2
α S cytosolic helical, 80 kDa	P78371	T-complex protein 1 subunit beta	174	13	4	4	535	57.5	6.46	1.9E+07	CCT2
α S cytosolic helical, 80 kDa	Q96QA5	Gasdermin-A	230	9	3	3	445	49.3	5.29	1.8E+07	GSDMA
α S cytosolic helical, 80 kDa	Q96AE4	Far upstream element-binding protein 1	16	7	3	3	644	67.5	7.61	1.8E+07	FUBP1
α S cytosolic helical, 80 kDa	P36551	Oxygen-dependent coproporphyrinogen-III oxidase, mitochondrial	215	11	4	4	454	50.1	8.25	1.7E+07	CPOX
α S cytosolic helical, 80 kDa	P48147	Prolyl endopeptidase OS=Homo sapiens	67	4	2	2	710	80.6	5.86	1.5E+07	PREP
α S cytosolic helical, 80 kDa	P22234	Multifunctional protein ADE2 OS=Homo sapiens	115	8	2	2	425	47	7.23	1.5E+07	PAICS
α S cytosolic helical, 80 kDa	P38117	Electron transfer flavoprotein subunit beta	170	7	2	2	255	27.8	8.1	1.4E+07	ETFB
α S cytosolic helical, 80 kDa	P13639	Elongation factor 2	179	10	6	6	858	95.3	6.83	1.3E+07	EEF2
α S cytosolic helical, 80 kDa	P07384	Calpain-1 catalytic subunit	238	6	3	3	714	81.8	5.67	1.3E+07	CAPN1
α S cytosolic helical, 80 kDa	P26038	Moesin	116	14	4	4	577	67.8	6.4	1.3E+07	MSN
α S cytosolic helical, 80 kDa	P08238	Heat shock protein HSP 90-beta	101	15	4	2	724	83.2	5.03	1.2E+07	HSP90AB1
α S cytosolic helical, 80 kDa	P62258	14-3-3 protein epsilon	247	13	3	2	255	29.2	4.74	1.2E+07	YWHAE
α S cytosolic helical, 80 kDa	O95302	Peptidyl-prolyl cis-trans isomerase FKBP9	103	3	2	2	570	63	5.08	1.2E+07	FKBP9
α S cytosolic helical, 80 kDa	P06576	ATP synthase subunit beta, mitochondrial	167	11	4	4	529	56.5	5.4	1.1E+07	ATP5B
α S cytosolic helical, 80 kDa	P32119	Peroxiredoxin-2 OS=Homo sapiens	244	27	3	3	198	21.9	5.97	1.1E+07	PRDX2
α S cytosolic helical, 80 kDa	P15311	Ezrin	127	11	3	3	586	69.4	6.27	1.1E+07	EZR
α S cytosolic helical, 80 kDa	Q04837	Single-stranded DNA-binding protein, mitochondrial	39	16	2	2	148	17.2	9.6	1.1E+07	SSBP1
α S cytosolic helical, 80 kDa	Q9BWD1	Acetyl-CoA acetyltransferase, cytosolic	132	14	3	3	397	41.3	6.92	1.0E+07	ACAT2

α S cytosolic helical, 80 kDa	P00505	Aspartate aminotransferase, mitochondrial	220	8	3	3	430	47.5	9.01	1.0E+07	GOT2
α S cytosolic helical, 80 kDa	P41250	Glycine--tRNA ligase	240	9	4	4	739	83.1	7.03	9.4E+06	GARS
α S cytosolic helical, 80 kDa	P19338	Nucleolin	178	11	6	6	710	76.6	4.7	8.2E+06	NCL
α S cytosolic helical, 80 kDa	Q00839	Heterogeneous nuclear ribonucleoprotein U	136	4	2	2	825	90.5	6	7.8E+06	HNRNPU
α S cytosolic helical, 80 kDa	Q99798	Aconitate hydratase, mitochondrial	225	4	2	2	780	85.4	7.61	7.8E+06	ACO2
α S cytosolic helical, 80 kDa	P34932	Heat shock 70 kDa protein 4	129	6	4	4	840	94.3	5.19	7.8E+06	HSPA4
α S cytosolic helical, 80 kDa	P26639	Threonine--tRNA ligase, cytoplasmic	148	3	2	2	723	83.4	6.67	7.8E+06	TARS
α S cytosolic helical, 80 kDa	Q96P63	Serpin B12 OS=Homo sapiens	152	11	4	4	405	46.2	5.53	7.8E+06	SERPINB12
α S cytosolic helical, 80 kDa	P30101	Protein disulfide-isomerase A3	159	4	2	2	505	56.7	6.35	7.4E+06	PDIA3
α S cytosolic helical, 80 kDa	P61604	10 kDa heat shock protein, mitochondrial	114	29	3	3	102	10.9	8.92	7.3E+06	HSPE1
α S cytosolic helical, 80 kDa	Q01813	ATP-dependent 6-phosphofructokinase, platelet type	104	6	2	1	784	85.5	7.55	5.1E+06	PFKP
α S cytosolic helical, 80 kDa	P26641	Elongation factor 1-gamma	4	5	2	2	437	50.1	6.67	5.0E+06	EEF1G
α S cytosolic helical, 80 kDa	O00154	Cytosolic acyl coenzyme A thioester hydrolase	224	6	2	2	380	41.8	8.54	4.9E+06	ACOT7
α S cytosolic helical, 80 kDa	Q96P16	Regulation of nuclear pre-mRNA domain-containing protein 1A	27	5	2	2	312	35.7	7.55	4.8E+06	RPRD1A
α S cytosolic helical, 80 kDa	P31150	Rab GDP dissociation inhibitor alpha	62	14	1	1	447	50.6	5.14	4.8E+06	GDI1
α S cytosolic helical, 80 kDa	Q9U142	Carboxypeptidase A4	9	7	2	2	421	47.3	6.7	4.7E+06	CPA4
α S cytosolic helical, 80 kDa	P50991	T-complex protein 1 subunit delta	38	5	2	2	539	57.9	7.83	4.2E+06	CCT4
α S cytosolic helical, 80 kDa	P22735	Protein-glutamine gamma-glutamyltransferase K	30	5	3	3	817	89.7	6.04	4.0E+06	TGM1
α S cytosolic helical, 80 kDa	Q08188	Protein-glutamine gamma-glutamyltransferase E	23	13	8	8	693	76.6	5.86	3.9E+06	TGM3
α S cytosolic helical, 80 kDa	P37837	Transaldolase OS=Homo sapiens	202	7	2	2	337	37.5	6.81	3.8E+06	TALDO1

α S cytosolic helical, 80 kDa	P08670	Vimentin	41	5	1	1	466	53.6	5.12	3.8E+06	VIM
α S cytosolic helical, 80 kDa	Q8NBF2	NHL repeat-containing protein 2	255	7	4	4	726	79.4	5.55	3.5E+06	NHLRC2
α S cytosolic helical, 80 kDa	P25786	Proteasome subunit alpha type-1	60	10	2	2	263	29.5	6.61	3.3E+06	PSMA1
α S cytosolic helical, 80 kDa	P09960	Leukotriene A-4 hydrolase	236	6	2	2	611	69.2	6.18	2.8E+06	LTA4H
α S cytosolic helical, 80 kDa	O43175	D-3-phosphoglycerate dehydrogenase	66	6	3	3	533	56.6	6.71	2.5E+06	PHGDH
α S cytosolic helical, 80 kDa	P16278	Beta-galactosidase	76	5	3	3	677	76	6.57	2.2E+06	GLB1
α S cytosolic helical, 80 kDa	O95757	Heat shock 70 kDa protein 4L	74	3	2	2	839	94.5	5.88	1.6E+06	HSPA4L
E. coli recombinant α S 14 kDa	P0DMV8	Heat shock 70 kDa protein 1A	23	49	34	17	641	70	5.66	2.6E+09	HSPA1B; HSPA1A
E. coli recombinant α S 14 kDa	P37840	Alpha-synuclein	26	69	16	12	140	14.5	4.7	1.3E+09	SNCA
E. coli recombinant α S 14 kDa	P11021	Endoplasmic reticulum chaperone BiP	20	19	9	9	654	72.3	5.16	2.0E+08	HSPA5
E. coli recombinant α S 14 kDa	P11142	Heat shock cognate 71 kDa protein	18	22	7	5	646	70.9	5.52	6.1E+07	HSPA8
E. coli recombinant α S 14 kDa	P38646	Stress-70 protein, mitochondrial	27	4	3	3	679	73.6	6.16	2.8E+07	HSPA9
E. coli recombinant α S 14 kDa	P0ACF8	DNA-binding protein H-NS	29	15	3	3	137	15.5	5.47	1.6E+07	hns
E. coli recombinant α S 14 kDa	P02452	Collagen alpha-1(I) chain	15	1	2	2	1464	138.9	5.8	9.1E+06	COL1A1
E. coli recombinant α S 14 kDa	Q86YZ3	Hornerin	8	3	2	2	2850	282.2	10.04	4.1E+06	HRNR
E. coli recombinant α S 14 kDa	P08123	Collagen alpha-2(I) chain	22	1	2	2	1366	129.2	8.95	3.0E+06	COL1A2

Mass spectrometry data of α S from HEK. The detailed procedure is described in the methods section. HEK293 α S C-term Strep II-tagged lysates were crosslinked and α S^H and α S^U were immunoprecipitated using StrepTrap 5ml columns. α S^H and α S^U were separated via size exclusion chromatography, run on a SDS-gel and gel pieces were lyophilized prior Mass spectrometry analysis. Lyophilized gel pieces were digested with trypsin. The quantification analysis was based on protein-specific peptides. For the mock sample, regular HEK293 were used. To further exclude false positive hits, recombinant α S^U was analyzed as well. The mock α S from regular HEK has a low abundance of α S, depicting α S^U remnants from HEK trapped in the StrepTap column. The α S from the 80 kDa gel piece exhibits 100 times more α S than the mock 80 kDa sample and the false discovery rate of proteins in these samples is 0.6 %. The E. coli 14 kDa band samples show several false positive hits including human HSP70. The data show that the most abundant protein in the α S^H sample except confirmed false positives is α S, strongly indicating a homo-oligomer.

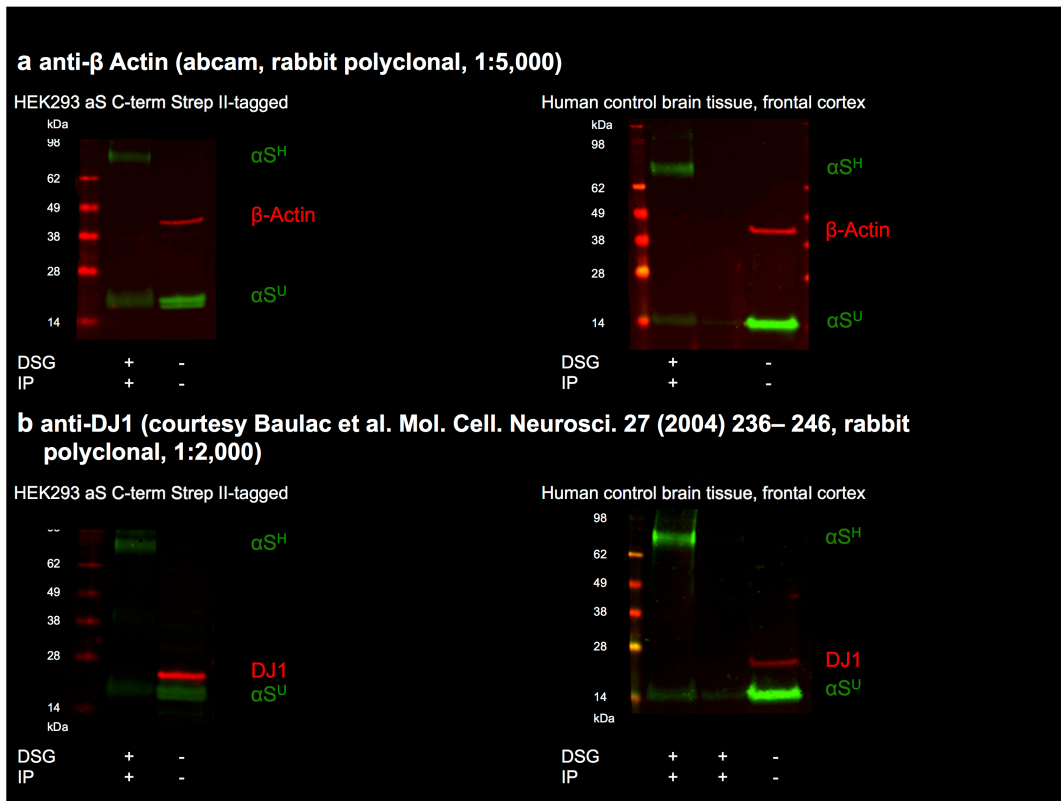


Fig. 8 Absent co-purification of β -Actin or DJ1 and α S^H. The crosslinking and immunoprecipitation procedures are described in the Methods section. Samples: HEK cells and human control brain tissue, frontal cortex. HEK293 α S C-term Strep II-tagged lysates were crosslinked and used to purify α S^H and α S^U using StrepTrap 5ml columns. The α S^H and α S^U from human brain lysate was immunoprecipitated after crosslinking using the Pierce™ Direct IP Kit. **a** Western blot of immunoprecipitated and crosslinked protein lysate from HEK cells and human brain in comparison to the original lysates demonstrating no co-immunoprecipitation of the β -Actin protein and α S^H. **b** Western blot of immunoprecipitated and crosslinked protein lysate from HEK cells and human brain in comparison to the original lysates demonstrating no co-immunoprecipitation of the DJ1 protein and α S^H. The immunoprecipitated human brain sample has been concentrated using an Amicon ultra 50 kDa filter unit and the first lane depicts the concentrated sample, second lane depicts the flow through. DSG “+“ = crosslinked sample. DSG “-“ = non-crosslinked (control) sample. IP “+“ = immunoprecipitated sample, IP “-“ = no immunoprecipitation performed.

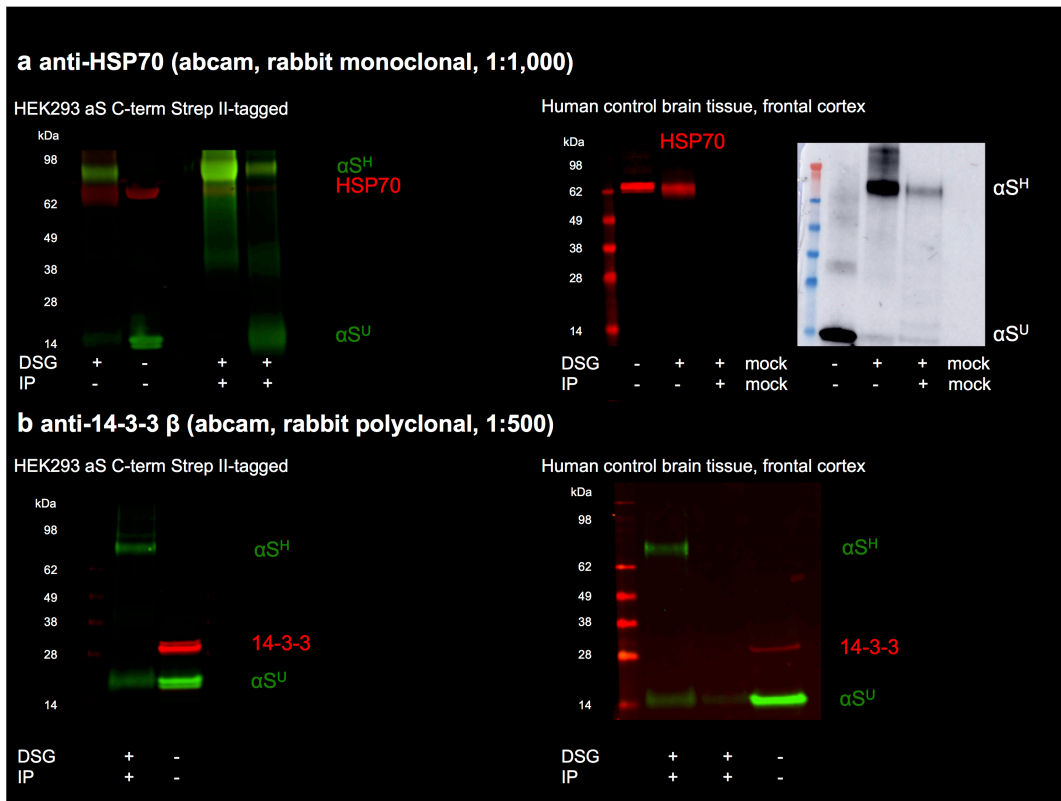


Fig. 9 Absent co-purification of HSP70 or 14-3-3 and α S^H. The crosslinking and immunoprecipitation procedures are described in the Methods section. Samples: HEK cells and human control brain tissue, frontal cortex. HEK293 α S C-term Strep II-tagged lysates were crosslinked and used to purify α S^H and α S^U using StrepTrap 5ml columns. The α S^H and α S^U from human brain lysate was immunoprecipitated after crosslinking using the Pierce™ Direct IP Kit. **a** Western blot of immunoprecipitated and crosslinked protein lysate from HEK cells and human brain in comparison to the original lysates and one mock IP sample (human brain, no antibody for capturing used). HEK: First lane depicts the crosslinked original lysate, second lane depicts the non-crosslinked original lysate, third and fourth lane depict the α S after crosslinking, immunoprecipitation and SEC to separate α S^H and α S^U. IP human brain samples have been concentrated using Amicon ultra 50 kDa filter units. The Western blots demonstrate no co-immunoprecipitation of HSP70 protein (left) and α S^H (right). **b** Western blot of immunoprecipitated and crosslinked protein lysate from HEK cells and human brain in comparison to the original lysates demonstrating no co-immunoprecipitation of 14-3-3 protein and α S^H. The immunoprecipitated human brain sample has been concentrated using an Amicon ultra 50 kDa filter unit and the first lane depicts the concentrated sample, second lane depicts the flow through. DSG “+” = crosslinked sample. DSG “-” = non-crosslinked (control) sample. IP “+” = immunoprecipitated sample, IP “-” = no immunoprecipitation performed.

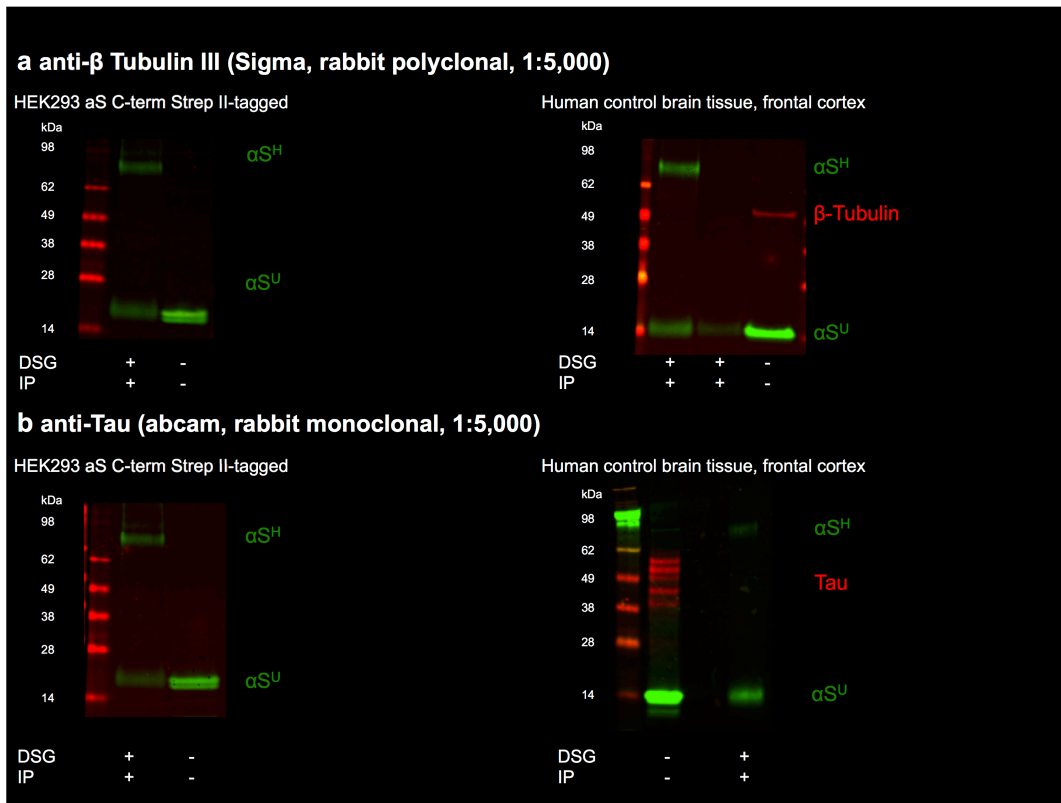


Fig. 10 Absent co-purification of β -Tubulin III or Tau and α S^H. The crosslinking and immunoprecipitation procedures are described in the Methods section. Samples: HEK cells and human control brain tissue, frontal cortex. HEK293 α S C-term Strep II-tagged lysates were crosslinked and used to purify α S^H and α S^U using StrepTrap 5ml columns. The α S^H and α S^U from human brain lysate was immunoprecipitated after crosslinking using the Pierce™ Direct IP Kit. **a** Western blot of immunoprecipitated and crosslinked protein lysate from HEK cells and human brain in comparison to the original lysates demonstrating no co-immunoprecipitation of β -Tubulin protein and α S^H in the brain sample. The immunoprecipitated human brain sample has been concentrated using an Amicon ultra 50 kDa filter unit and the first lane depicts the concentrated sample, second lane depicts the flow through. β Tubulin could not be demonstrated in the original lysate and immunoprecipitated sample of HEK cells. **b** Western blot of immunoprecipitated and crosslinked protein lysate from HEK cells and human brain in comparison to the original lysates demonstrating no co-immunoprecipitation of tau protein and α S^H in the human brain sample. Tau could not be demonstrated in the original lysate and immunoprecipitated sample of HEK cells. DSG “+“ = crosslinked sample. DSG “-“ = non-crosslinked (control) sample. IP “+“ = immunoprecipitated sample, IP “-“ = no immunoprecipitation performed.

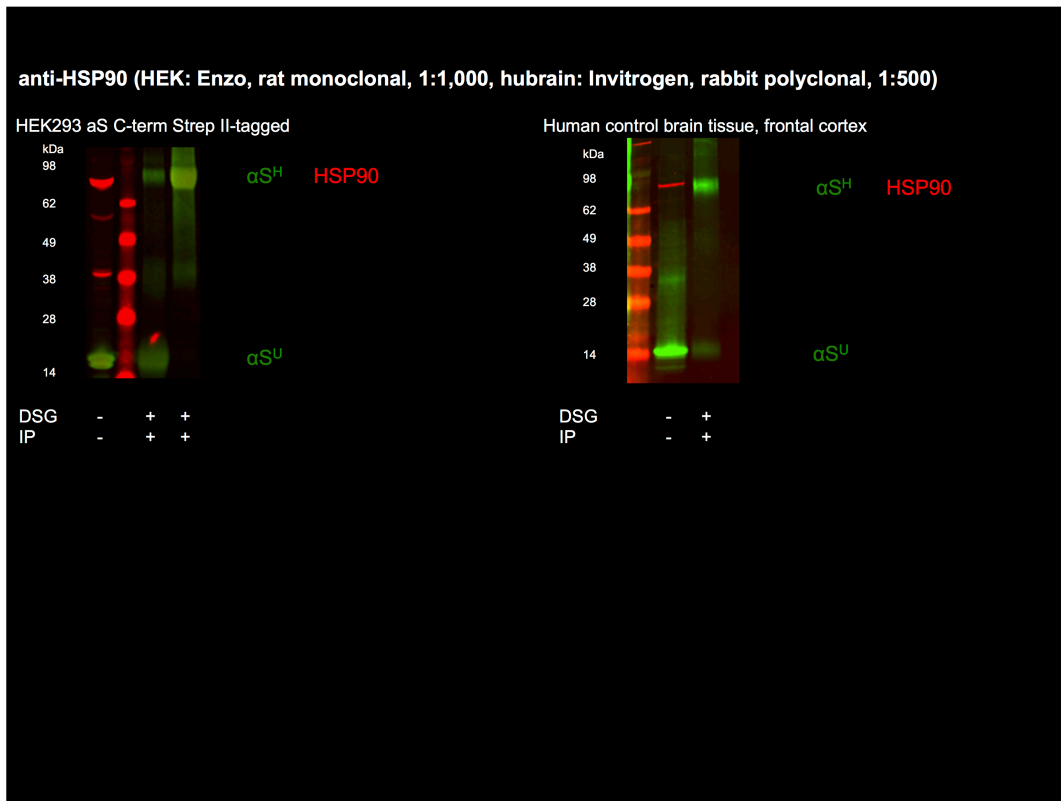


Fig. 11 Absent co-purification of HSP90 and α S^H. The crosslinking and immunoprecipitation procedures are described in the Methods section. Samples: HEK cells and human control brain tissue, frontal cortex. HEK293 α S C-term Strep II-tagged lysates were crosslinked and used to purify α S^H and α S^U using StrepTrap 5ml columns. The α S^H and α S^U from human brain lysate was immunoprecipitated after crosslinking using the Pierce Pierce™ Direct IP Kit. Western blot of immunoprecipitated and crosslinked protein lysate from HEK cells and human brain in comparison to the original lysates demonstrating no co-immunoprecipitation of HSP90 protein and α S^H. HEK: First lane depicts the non-crosslinked original lysate, second lane and third lane depict the α S after crosslinking, immunoprecipitation and SEC to separate α S^H and α S^U. DSG “+“ = crosslinked sample. DSG “-“ = non-crosslinked (control) sample. IP “+“ = immunoprecipitated sample, IP “-“ = no immunoprecipitation performed.

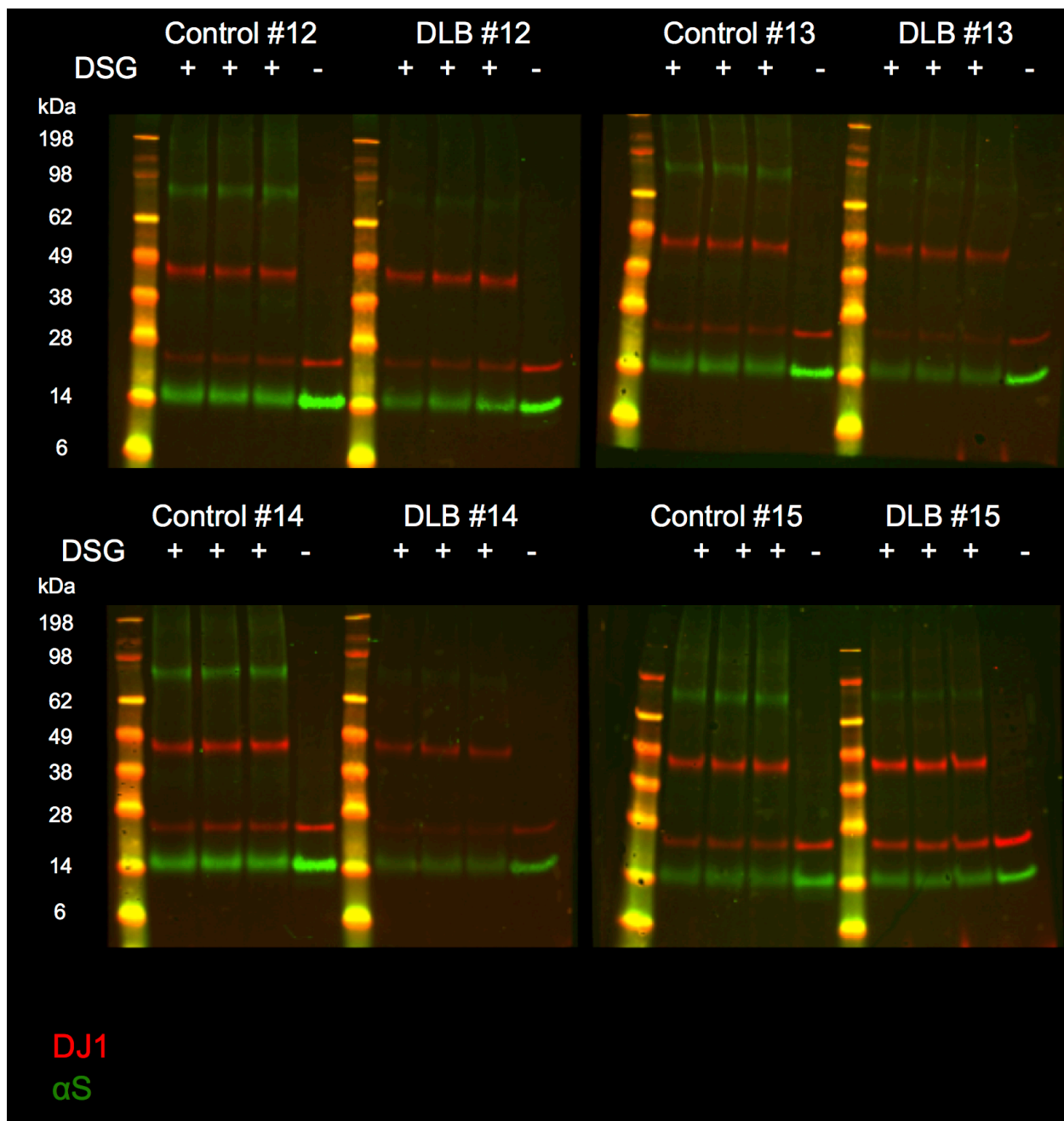


Fig. 12 Exemplary Western blot of analyzed samples. Western blot of crosslinked frontal cortex (FC) lysate (control vs. DLB, frontal cortex, n=4 each). The crosslinking reaction was performed in technical triplicates alongside with one non-crosslinked (PBS) sample. The Western blot demonstrates reduced α S^H / α S^U ratios in DLB patients compared to controls. DSG “+” = crosslinked sample. DSG “-” = non-crosslinked sample. Green = α S, red = DJ1

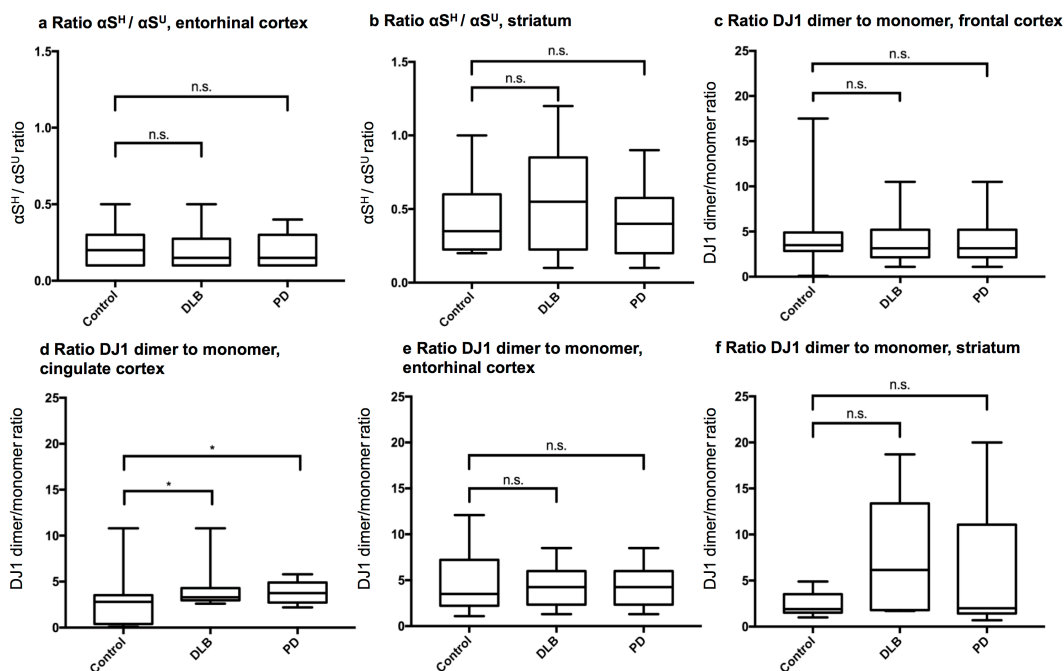


Fig. 13 Similar $\alpha S^H / \alpha S^U$ and DJ1 dimer to monomer ratios across different brain regions. **a** No significant alteration of the $\alpha S^H / \alpha S^U$ equilibria in the entorhinal cortex comparing controls (n = 7) to PD (n = 6) and DLB (n = 6) patients. **b** No significant alteration of the $\alpha S^H / \alpha S^U$ equilibria in the striatum comparing controls (n = 6) to PD (n = 6) and DLB (n = 4) patients. The DJ1 serves as an internal control for the crosslinking procedure. Across different brain regions (**c** frontal cortex **e** entorhinal cortex, **f** striatum) no differences in DJ1 dimer to monomer ratios were detected comparing controls, DLB patients and PD patients. **d** PD and DLB patients exhibited increased DJ1 ratios in the cingulate cortex ($p < 0.01$). Thus, higher $\alpha S^H / \alpha S^U$ are not due to an overcrosslink of the samples as DLB and PD samples stay low in their $\alpha S^H / \alpha S^U$ ratios. Entorhinal cortex controls n=7 individuals, DLB n=6 individuals, PD n=6 individuals. Cingulate cortex controls n=7 individuals, DLB n=7 individuals, PD n=6 individuals. Frontal cortex controls n=19 individuals, DLB n=14 individuals, PD n=8 individuals. Striatum controls n=6 individuals, DLB n=4 individuals, PD n=6 individuals. Samples have been analyzed in biological duplicates and technical triplicates. N.s.=not significant.

summary variance analysis, frontal cortex, ratio $\alpha S^H / \alpha S^U$ vs. McKeith staging

	Df	Sum Sq	Mean Sq	F value	Pr(>F)
McKeith	1	1.549	1.5490	33.23	8.14e-08 ***
Residuals	106	4.941	0.0466		

Signif. codes: 0 '***' 0.001 '**' 0.01 '*' 0.05 '.' 0.1 ' ' 1

summary variance analysis, cingulate cortex, ratio $\alpha S^H / \alpha S^U$ vs. McKeith staging

	Df	Sum Sq	Mean Sq	F value	Pr(>F)
McKeith	1	0.1045	0.10446	6.209	0.0172 *
Residuals	38	0.6393	0.01682		

Signif. codes: 0 '***' 0.001 '**' 0.01 '*' 0.05 '.' 0.1 ' ' 1

summary variance analysis, entorhinal cortex, ratio $\alpha S^H / \alpha S^U$ vs. Braak Tau (neurofibrillary tangle, NFT) staging

	Df	Sum Sq	Mean Sq	F value	Pr(>F)
Braak NFT	1	0.0670	0.06702	4.82	0.0347 *
Residuals	36	0.5006	0.01391		

Signif. codes: 0 '***' 0.001 '**' 0.01 '*' 0.05 '.' 0.1 ' ' 1

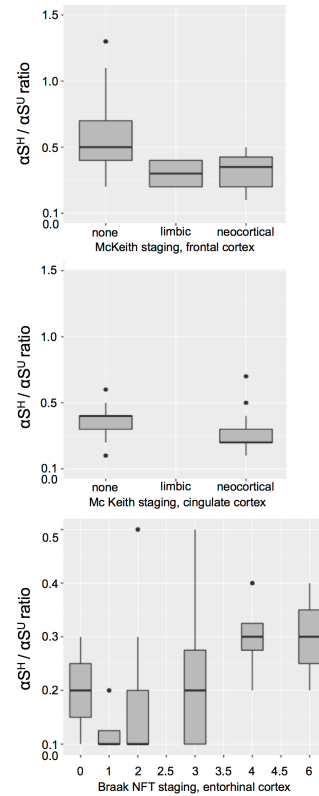


Fig. 14 Significant difference of decreased $\alpha S^H / \alpha S^U$ ratios and increased McKeith staging (none, limbic, neocortical) of the frontal cortex and cingulate cortex. Significant difference of decreased $\alpha S^H / \alpha S^U$ ratios and increased Braak neurofibrillary tangle (NFT) staging in the entorhinal cortex.

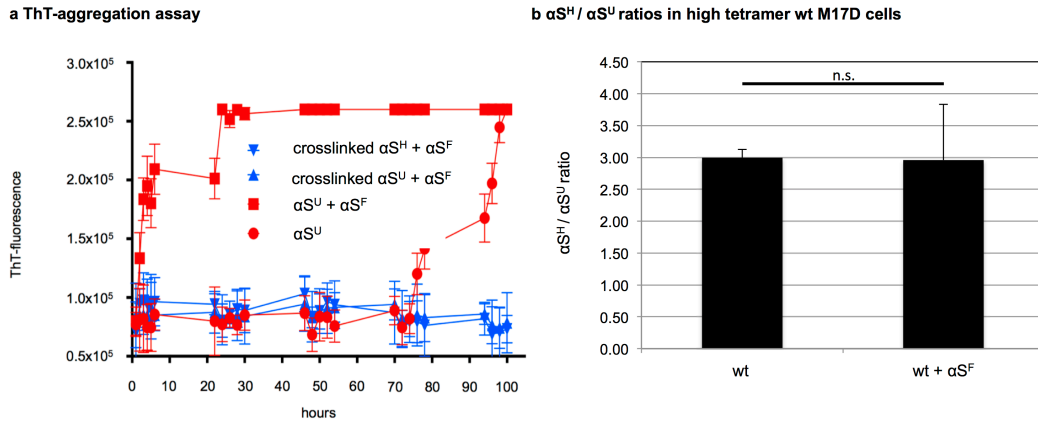


Fig. 15 a ThT-aggregation assay of recombinant αS^U and crosslinked brain-derived αS^U and αS^H . Comparison between non-crosslinked and crosslinked αS species in a Thioflavin T-aggregation assay. Crosslinked brain-derived αS^U and αS^H show an absence of insoluble αS formation, with or without seeding of recombinant αS^F (αS : αS^F 500,000:1). Non-crosslinked recombinant αS^U will slowly form ThT-positive fibrils, greatly accelerated by the addition of αS^F (αS : αS^F 500,000:1) under otherwise identical conditions. **b** αS^F -seeded M17D high tetramer cell lines maintain $\alpha S^H / \alpha S^U$ ratios in wt cells, indicating that amyloid aggregation itself does not stimulate αS^H destabilization.